VOL. 20, NO. 2, 2021, 19-24
www.elektrika.utm.my
ISSN 0128-4428

ELEKTRIKA
Journal of Electrical Engineering

Development of *XY* Micro-Position Stage Based on a Shape Memory Alloy

Alaa Abu Zaiter

[1]Faculty of Applied Engineering and Urban Planning, University of Palestine (UP), Gaza, Palestine.

Corresponding author: a.zaiter@up.edu.ps

Abstract: This paper reports a novel monolithic two DoF micro-positioning stage using shape-memory-alloy (SMA) actuator. The design was fabricated in a one fabrication step and it comprises all actuation functions in a single piece of SMA. The square shaped actuator has dimensions of 10 mm × 10 mm × 0.25 mm. The device includes a moving stage in the center which is connected to four SMA springs to generate large displacement in two directions, *x*- and *y*- axes. The four SMA actuators underwent annealing process using internal joule heating by flowing electrical current through the springs. Each of SMA springs has been actuated individually by internal joule heating generated using an electrical current. The developed design has been simulated to verify thermal response and heat distribution. In addition, the micro-positioning stage was experimentally tested. The maximum displacement results of the stage are 1.1 mm and 1.1 mm along the directions of *x*- and *y*- axes, respectively. The developed micro-positioning stage has been successfully demonstrated to control the position of a small object for microscopic imaging applications.

Keywords: Actuator, Micro-positioning stage, Shape-memory-alloy (SMA), SMA spring.

Article History: received 25 May 2021; accepted 12 June 2021; published 28 August 2021.

1. INTRODUCTION

The micro-positioning stage is a promising element in the future of micro technologies. Nowadays, it is widely used in many areas such as in atomic force microscopy [1], micro- and nano-surgical tools [2], maskless lithography [3], scanning in microscopy [4] and biomedical application. Generally, a micro-positioning machine involves a stage that moves in several degrees of freedom (DoF) and it can move accurately up to micron and submicron resolutions. The researchers in the area of micro-positioning devices are continuously looking to increase the device resolution and its working space range. Moreover, simplification of the control methods, minimizing the size and decreasing the response time are of the researcher's interest. These characteristics can be achieved by improving the structure of the design and actuating methods of the stage. The researchers have reported various methods to actuate micro-position stage. One of these actuators is a piezoelectric-actuator which is commonly used due to its high resolution, large actuation force, and low power consumption [5]. Usually, in the piezoelectric micro-position design, flexure-based structures are used. The advantages of this structure is backlash-free movement, low friction, and no requirements for lubrication [6]. The design and driving of flexure-based structures has been divided into two methods namely series kinematic motion and parallel kinematic motion. [7]. Nevertheless, the piezoelectric-driven of micro-positioning stages have a limited range of displacement. In addition, the control of piezoelectric actuators is complicated due to its significant hysteresis, which requires a complex numerical modeling and algebraic solutions [8].

Another actuation method used in micro-positioning stages is electrostatic that has a fast response time. However, it suffers a very limited displacement range. Consequently, many researches have been reported increased displacement range. Olfatnia et al. [9]. In addition, the operating of the electrostatic actuator needs high voltage. Also, its fabrication processes are complicated.

Electromagnetic micro-positioning stage is another actuation method used for achieving higher displacements [10]. In addition, the use of electromagnetic actuators offers more advantages such as fast response, movements without friction and linearly displacement. Nonetheless, the fabrication of electromagnetic micro-positioning stages is considered complex and expensive. Furthermore, their size is unacceptable for some applications in biomedical field [11].

The micro-positioning stages can be also driven by electrothermal actuators based on a bimorph actuation mechanism. This mechanism requires low voltage compared with other actuators methods. In addition, it shows a higher displacement and an actuation high force [12]. Despite these advantages, this method generally has low response time and it needs high working temperatures which unsuitable for some applications [13].

Overall, the previous actuation methods, shape memory alloy (SMA) actuator shows a great potential in micro-

position stage because it has exceptional properties compared with other actuation methods such as high work density, high mechanical robustness and large range of displacement [14]. Furthermore, the SMA material is biocompatible material which is considered an important issue in many applications especially in biomedical area [13, 15]. Many researches have been done in micro-positioning stages driven by SMA actuators but still many features of this material are not fully utilized. For instance, a previous research by Buchaillot et al. [16] reported a micro-positioning device based on a sputtered SMA actuator but still suffers from low actuation force. Other work has utilized SMA springs that connected with middle stage to develop two DoF micro-positioning stage [17]. However, the device is considered bulky due to the many SMA Springs and other materials to assemble the positioning Stage. Also, Padhan et al. [18] developed XY Positioning Stage using four SMA spring actuator with high actuation range. Nevertheless, the device is considered large in size, not suitable for limited area and needs multiple fabrication steps. Consequently, the above-mentioned researches still limited in complexity and costly fabrication process. These issues will be addressed in this work.

This paper reports the development of a novel monolithic *XY* micro-positioning stage driven by SMA actuators. The developed design consists of four SMA actuator springs that provide the stage with a linear movement in *x*- and *y*- axes. The actuating SMA springs are controlled by internal joule heating. The internal heating circuit controls the current flow inside the SAM spring by pulse-width modulated (PWM) signal. The important characteristic of this developed micro-position stage is being fabricated from a single piece of SMA material with one step fabrication process. This simple fabrication process allows economical fabrication, smaller device size and promote the device robustness. In addition, this fabrication method enables further miniaturization of the SMA based device. The paper presents the thermal response and the heat distribution of the device using the finite element analysis (FEA). Furthermore, an explanation of the design of the heating circuit, fabrication and annealing process are provided in this paper. Lastly, the results of this experiment and the possible future applications are presented.

2. DESIGN AND WORKING PRINCIPLE

The design consists of an SMA stage located at the middle of the device and connected to four SMA springs at each of its sides. Subsequently, these springs are linked to an outer square shield that completes the structure of the device. The widths of each SMA spring is 200 µm. In addition, each spring connected in the middle with a copper wire for individual heating purposes. The moving stage is square and it has dimensions of 2 mm × 2 mm. The overall structure has dimensions of 10 mm × 10 mm with a thickness of 250 µm as shown in Figure 1. The working principle of the device is based on the actuation of these four springs. Two springs are responsible for the stage movement in *x* direction. For instance, the right spring pulls it along positive *x*-axis whilst the left spring attracts it along the opposite direction.

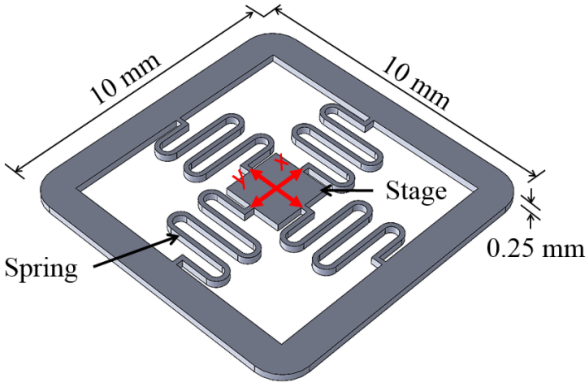

Figure 1. The design of the micro-positioning *x*-*y* stage.

Similarly, the upper and lower springs carry out the movement along the positive and negative *y*-axis, respectively. Moreover, the stage can move along both *x*- and *y*-axes when *x*- and *y*-axes springs are actuated at the same time. Each SMA spring is trained by annealing process so it memorizes a contracted form once heated beyond the threshold 'austenite' temperature. At the same time, each spring is easily allowed to extend at lower temperatures (at martensite phase) when pulled by heated springs. Each SMA spring can be individually activated by means of Joule heating induced by DC current. The SMA actuators are controlled using a pulse-width modulated (PWM) signal that controls the electrical current flow in the heating circuit. The heating distribution is simulated and presented the thermal response to supplied currents (1A – 5A).

3. SIMULATION

This section presents the simulation results of the SMA actuators. It has been done using COMSOL Multiphysics software to proof the working principle of the device that discussed in the above section. The requirements of SMA material properties that set in the simulation software are provided in Table 1. The simulation investigates the thermomechanical behavior which consists of thermal response, heat distribution and internal joule heating of SMA springs. Additionally, the simulation evaluated different currents range from 1A to 5A applied to the SMA spring. This analysis will enable the selection of the optimum current values for actuation and the annealing process for the SMA springs.

In the simulation, the current supply for SMA spring was set from the middle of the spring and the ground connect the outer square shield of the device. The results in the first simulation part (Figure 2(a)) depicts the heat distribution along with SMA spring. The current supply was 2A and the maximum temperature was ~105 °C along the spring. Figure 2(b) shows the SMA spring internal heating response for different current supply range from 1A to 5 A, and it plots the thermal response for the first 10 second for each current value. The Figure shows the higher temperature obtained for higher current applied. The minimum temperature value was ~ 41 °C when the current

applied is 1 A whereas the maximum temperature was ~610 °C when the current was set to 5 A.

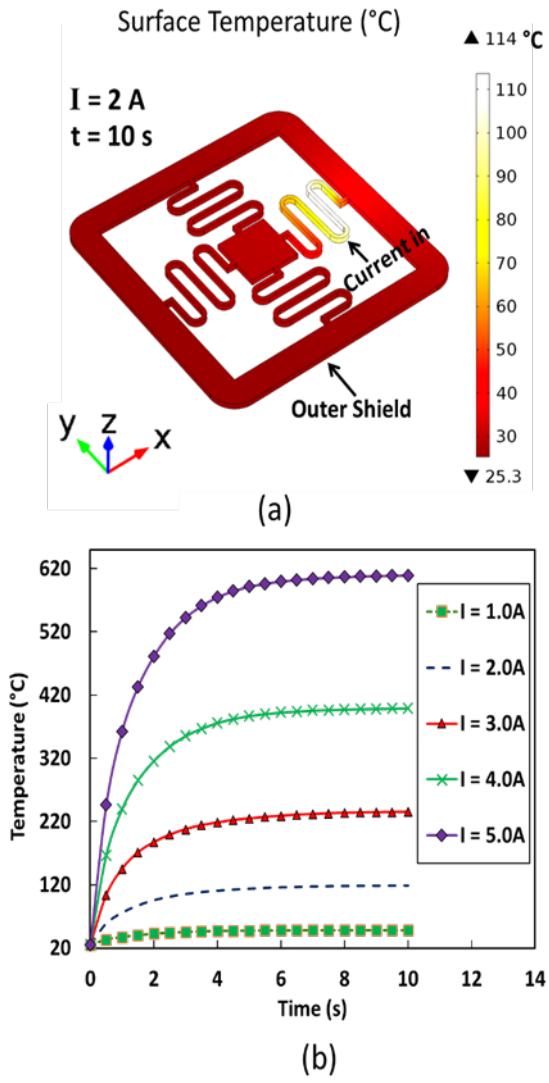

Figure 2: Simulation results of the SMA springs; (a): Perspective view of Joule heating distribution, (b): Joule heating response to different supplied currents.

From the previous results, it is observed that when one of SMA spring was heated to be actuated there was no heat influence on the other SMA springs and the moving stage. This advantage enhances single annealing process for each SMA spring without any effect on the other SMA springs. At the same time, it enables the individual actuation of the SMA springs. Furthermore, the simulation results can be assumed to select the suitable current supply for annealing process (which requires a minimum temperature of 350 °C) and for actuating process (i.e., bringing their SMA temperature beyond the austenitic temperature of 65 °C) are 2 and 4 A, respectively.

Table 1. The thermomechanical properties of SMA [19]

Properties	SMA
Coefficient of thermal expansion (1/K)	6.6×10^{-6} (martensite phase) 11×10^{-6} (austenite phase)
Density (kg/m^3)	6450
Electrical conductivity (S/m)	11×10^5 - 12.5×10^5
Heating capacity J/(kg·K)	390
Young's modulus (Pa)	20.6×10^9 – 70.33×10^9
Thermal conductivity (W/(m·K))	10
Poisson's ratio	0.33

4. FABRICATION AND ANNEALING PROCESSES

The device was formed from bulky SMA sheet (SAES Mermry, Germany) with thickness of 250 µm and austenitic temperature of SMA sheet is 65 °C. The fabrication process has been done by one fabrication step using wire-micro-electrical-discharge-machining (Wire-µEDM) of the SMA sheet (Figures 3a and 3b). Then the device is ready for annealing (training) process which has been done independently for each SMA springs to memorize the compressed shape. To start the annealing process, the SMA springs were hold in compressed shape and the temperature of SMA spring was increased to around 400 °C for 15 to 20 minutes (Figure 3c). Internal joule heating circuit was used to increase the temperature of the springs by passing the electrical current through the SMA spring. The heating circuit contains the microcontroller that programed to control four PWM signals for each SMA. The PWM circuit controls the current flow through the springs. Each SMA spring was connected between the heating circuit and SMA using copper wires (50-µm-diameter) as shown in the (Figure 3d). To avoid oxidization of SMA material during the annealing process, it was done in nitrogen surroundings. The power source was set to supply 2 A and 10 V.

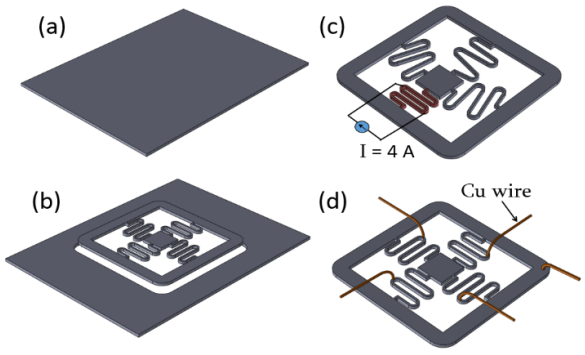

Figure 3: Fabrication and training process; (a): SMA sheet, (b): The µEDM-ed device, (c): Annealing process, (d): The final device with Cu lead wires.

5. EXPERIMENTAL RESULTS AND DISCUSSION

This section presents the experimental results and the discussion of the developed SMA micro-positioning stage. Starting with micro-positioning actuation functional tests followed by testing the temporal response of SMA springs and measuring the displacement of the actuation range in *x*- and *y*- axes. Next, the heat distribution and thermal response during the actuation of SMA springs were tested using the thermal camera. Furthermore, application of moving the *x*-*y* stage under microscopy is also demonstrated.

5.1 Stage Actuation Tests

In this part, the developed micro-positioning stage was tested by actuating the SMA springs to move the middle stage in the *x*- and *y*-axes directions. To start the test of micro-position stage, the stage was set in the initial state without actuation (Figure 4a). The stage moves in positive *y*-axis direction by actuation of the upper spring as shown in Figures 4b. To be moved in negative *y*-axis direction the lower spring was actuated (Figure 4c). Also, the stage can be moved in positive and negative *x*-axis by actuating the left and right springs. Moreover, two springs can be actuated at the simultaneously to achieve movement in *x*- and *y*-axes directions (Figures 4d). Torsional actuation of the stage is also possible by adding additional SMA spring in all side of the stage.

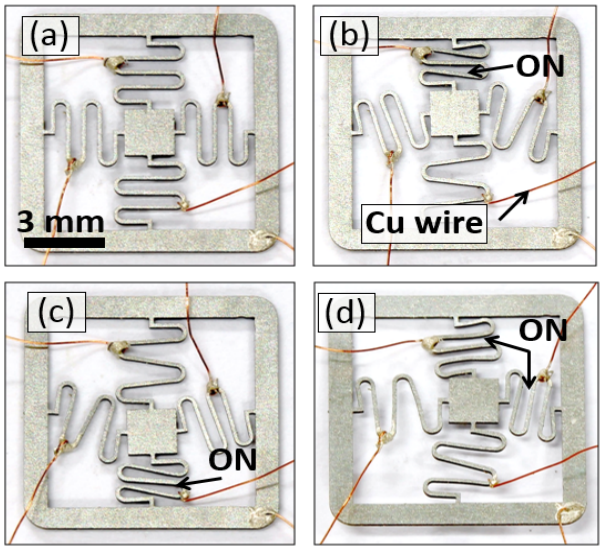

Figure 4: The developed x-y stage in motion; (a): initial state, (b): Upper spring actuated; (c): Lower spring actuated; (d): Upper and right springs actuated.

5.2 Temporal displacement response of the micro positioning stage

The experimental setup as shown in Figure 5 has been used to characterize the displacement range and thermal responses of the developed micro-positioning stage. The heating circuit was used to activates each SMA spring. As well, two laser displacement sensors (LK-G32, Keyence, IL, USA) were fixed to measure the displacement range in *x*- and *y*-axes directions. While the thermal (IR) camera (Jenoptik VarioCam HD 5M, Jena, Germany) is utilized to measure the temperature response of micro-positioning stage.

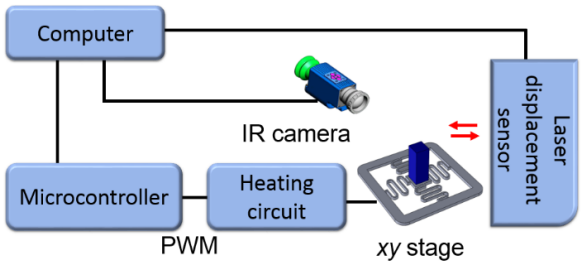

Figure 5: Experimental setup of the *x*-*y* stage for characterization.

Figure 6 plots temporal responses of displacement and temperature response of *y*-axis springs. The actuation cycle was done in 16 second to realize the highest and lowest displacement range along *y*-axis. The 100% duty cycle of PWM signal was applied during the actuations cycle of two springs (upper and lower springs). The movement stage was set in initial state. Firstly, the upper spring was activated for 6 seconds to move the middle stage in the positive *y*-axis. The highest displacement of ~596 µm was achieved in 2.2 second. During the actuation of upper spring, the maximum temperature of the upper and lower SMA springs measured to be 130 °C and 25 °C, respectively. Next, the lower spring was activated for 6 second after the deactivation of upper spring. This resulted in the movement of the middle stage in negative *y*-axis direction to reach the maximum displacement of ~624 µm in ~2.3 second. Furthermore, for activation of lower spring the temperature was increased to 132 °C and the temperature of upper spring was reduced to 25 °C. These results match well with the simulation results as described in Section 3.

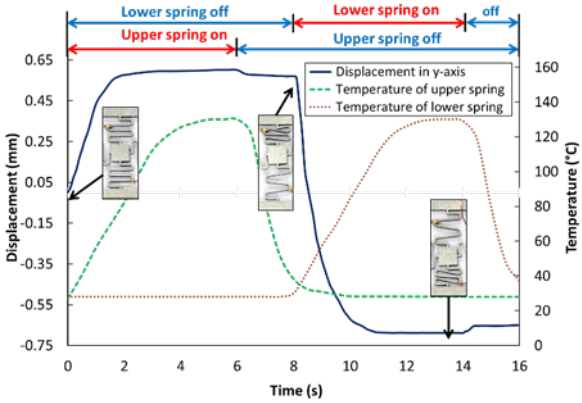

Figure 6: Stage displacement and temperature response of *y*-axis springs.

5.3 Thermal characterization of the devices

This section presents the results of thermal response during the actuation of SMA springs for the developed micro-position stage. In addition, the heat disruption and temperature values along the SMA spring are investigated.

These results used to prove that SMA springs can be actuate and annealed individually without affecting other SMA springs. The experimental setup was described before (Section 5.2). Figure 7 shows the thermal response for SMA spring during activation and deactivation for 5 seconds for each stage. Moreover, it shows the thermal imagining using IR camera for SMA spring during this cycle. There are five measurement points for the temperature response and used to plot the graph. *Point 1* is located in the movement stage and *P5* at the outer shield while *Point 2*, *Point 3* and *Point 4* are set along the spring. The plot of these points shows significant difference in temperature values along SMA spring. The *Point 3* and *Point 4* are near the current supplying point so they show the highest temperature of ~125 °C while P2 is ~65 °C. These values are considered enough for actuation the SMA spring as the temperature values are above the austenitic temperature. On the other hand, the temperature of *Point 1* and *Point 5* in the movement stage and the outer shield are increased slightly from room temperature to reach 33 °C and 40 °C, respectively. These results prove that there is no transmission of heat from spring to the moving stage and the outer shield. Furthermore, the thermal images in Figure 7 shows the temperature distribution during the activation and deactivation of the lower spring. These outcome results are obviously well matched with the simulation results as described in Section 3.

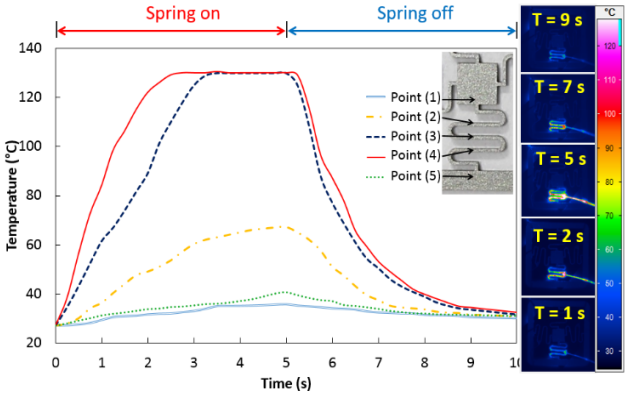

Figure 7: Temperature profile of the lower spring's heating response while actuating.

5.4 Application of the micromanipulator

The micro-position sages could be utilized for micro-manipulation applications. This section focuses on testing the developed micro-position sages to manipulate the small object under microscopic imaging. The aims of this application to show the possibly of control of the position of micro-object (micro-gear) under a microscope. The micro-scanning of the gear was snaped during the manipulation. At the beginning, the gear was fixed in the center of the stage (Figure 8a). when left spring was activated the gear moved to the negative *x*-axis (Figure 8b). Another example, the gear was moved along the positive *x*- and *y*-axes by actuating the upper and right springs simultaneously (Figure 8c).

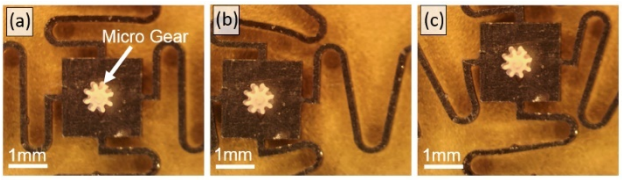

Figure 8: Application of the xy stage in motion (under microscope); (a): Stage in center position, (b): left spring actuated, (c): Upper spring actuated.

6. CONCLUSION

This paper presented a novel monolithic two DoF micro-positioning stage driven by shape-memory-alloy (SMA) actuator. The micro-positioning stage provide 2 DoF along with *x*- and *y*-axes directions, it has been done by controlling the four SMA springs. The developed device was monolithically realized in a single fabrication step from SMA sheet, which integrate all device function in a single piece of SMA. This enables economical fabrication, smaller device size and promote the device robustness. In addition, this way of fabrication method enables more miniaturization of the device. The individual annealing process has been done for each SMA springs to memorize the compressed shape. This process has been done by individual internal joule heating by supply electrical current through each SMA spring. Moreover, the thermal response and heat distribution of SMA spring was investigated by simulation and experimental tests. As well as, the high temperature changes through the four SMA springs don't affect the temperature of the moving stage. This will make this device suitable to be used for moving small objects. The maximum displacement results of the stage are 1.1 mm and 1.1 mm along the directions of *x*- and *y*- axes, respectively. Controlling the stage by PWM signal was verified to be effective in accomplishing diverse stage displacements. Miniaturization of this device is possible so it can achieve smaller displacements if needed. On the other hand, the device also can be extended to achieve higher displacements. Future work of this device can focus on increasing the accuracy of the displacement by developing more sophisticated control circuit. Moreover, new springs can be added to the design to facilitate torsional movement.

REFERENCES

[1] S. Vahabi, B.N. Salman and A. Javanmard, "Atomic force microscopy application in biological research: a review study," *Iranian journal of medical sciences*, vol. 38, no. 2, p. 76, 2013.

[2] J. Wang and S. Guo, "Development of a precision parallel micro-mechanism for nano tele-operation," *International Journal of Robotics and Automation*, vol. 23, no. 1, pp. 56-63, 2008.

[3] Y. Ihn, S. Ji, H. Moon, H-R. Choi and J. Koo, "A dual step precision multi-DOF stage for maskless digital lithography," *Microsystem Technologies*, vol. 18, no. 9-10, pp. 1741-1750, 2012.

[4] A. J. Fleming, "Dual-Stage Vertical Feedback for High-Speed Scanning Probe Microscopy," *Control*

Systems Technology, IEEE Transactions, vol. 19, no. 1, pp. 156-165, 2011.

[5] J. Li, H. Huang and T. Morita, "Stepping piezoelectric actuators with large working stroke for nano-positioning systems: a review," *Sensors and Actuators A: Physical*, vol. 292, pp. 39-51, 2019.

[6] K. Cai, Y. Tian, F. Wang and D. Zhang, "Development of a piezo-driven 3-DOF stage with T-shape flexible hinge mechanism," *Robotics and Computer-Integrated Manufacturing*, vol. 37, pp. 125-138, 2016.

[7] Z. Guo, Y. Tian and X. Liu, "Design and control methodology of a 3-DOF flexure-based mechanism for micro/nano-positioning," *Robotics and Computer-Integrated Manufacturing*, vol. 32, pp. 93-105, 2015.

[8] P-Z. Li, D-F. Zhang, B. Lennox and F. Arvin, "A 3-DOF piezoelectric driven nanopositioner: Design, control and experiment," *Mechanical Systems and Signal Processing*, vol. 155, pp. 107603, 2021.

[9] M. Olfatnia, L. Cui, P. Chopra and S. Awtar, "Large range dual-axis micro-stage driven by electrostatic comb-drive actuators," *Journal of Micromechanics and Microengineering*, vol. 23, no. 10, pp. 105008, 2013.

[10] S. Xiao and Y. Li, "Optimal design, fabrication, and control of an micropositioning stage driven by electromagnetic actuators," *Industrial Electronics, IEEE Transactions*, vol. 60, no. 10, pp. 4613-4626, 2013.

[11] H. Zhang, Z. Wu and Q. Xu, "Design of a New XY Flexure Micropositioning Stage with a Large Hollow Platform. in Actuators," Multidisciplinary Digital Publishing Institute, 2020.

[12] U. Izhar, A. Izhar and S. Tatic-Lucic, "A multi-axis electrothermal micromirror for a miniaturized OCT system," *Sensors and Actuators A: Physical*, vol. 167, no. 2, pp. 152-161, 2011.

[13] S. Afrang, H. Mobki, M. Hassanzadeh and G. Rezazadeh, "Design and simulation of a MEMS analog micro-mirror with improved rotation angle," *Microsystem Technologies*, vol. 25, no.3, pp. 1099-1109, 2019.

[14] A. AbuZaiter, M. Nafea and M. S. M. Ali, "Development of a shape-memory-alloy micromanipulator based on integrated bimorph microactuators," *Mechatronics*, 38: p. 16-28. 2016.

[15] A. AbuZaiter, O. F. Hikmat, M. Nafea and M. S. S. Mohamed Ali, "Design and fabrication of a novel XYθz monolithic micro-positioning stage driven by NiTi shape-memory-alloy actuators," *Smart Materials and Structures*, vol. 25, no. 10, pp. 105004, 2016.

[16] L. Buchaillot, et al., "Thin Film of Titanium/Nickel Shape Memory Alloy for Multi-Degree of Freedom Microactuators," 生産研究, vol. 51, no. 8, pp. 642-643, 1999.

[17] D. Singh, R. Choudhury, Y. Singh and M. Mukherjee, "Workspace analysis of 3-DOF U-shape base planar parallel robotic motion stage using shape memory alloy restoration technique (SMART) linear actuators," *Applied Sciences*, vol. 3, no. 4, pp. 1-22, 2021.

[18] A. Padhan and Y. Singh, "Design and Development of a XY Positioning Stage Using Shape Memory Alloy Spring Actuator, in Recent Advances in Mechanical Engineering," *Springer*, pp. 593-600, 2021.

[19] A. AbuZaiter and M. S. M. Ali. "Analysis of thermomechanical behavior of shape-memory-alloy bimorph microactuator," *5th International Conference on Intelligent Systems, Modelling and Simulation*. *IEEE*, 2014.